Combined FDTD/Macromodel Simulation of Interconnected Digital Devices

S. Grivet-Talocia, I. S. Stievano, I. A. Maio, F. G. Canavero
Dip. Elettronica, Politecnico di Torino, Torino, Italy
(E-mail: grivet@polito.it)

Abstract

Behavioral models of digital devices based on Radial Basis Functions (RBF) are incorporated into a Finite-Difference Time-Domain (FDTD) solver for full-wave analysis of interconnected drivers and receivers. This modeling strategy allows a very accurate and efficient full-wave solution of interconnection structures with possibly complex geometry including the nonlinear and dynamic effects of real-world digital devices, without the need of detailed transistor-level models. Examples of signal integrity and field coupling analysis are shown.

1. Introduction

The high complexity of modern electronic systems requires careful modeling strategies at early stages of the design process. This is particularly important for the characterization of interconnected structures loaded by digital drivers and receivers. Indeed, it is well known that Electromagnetic Compatibility (EMC) and Signal Integrity (SI) are strongly affected by the geometry of the interconnects and by the possibly complex nonlinear/dynamic behavior of the electronic devices collocated at their terminations. An accurate solver must combine a rigorous full-wave scheme together with precise models of digital ports.

Two main approaches for the simulation of a loaded interconnected structure can be devised. Their suitability depends on the particular type of analysis that is considered, as briefly described in the following paragraphs.

The first option is to retain the full complexity of the components using their transistor-level model, attempting the derivation of simple macromodels for the description of the signal propagation paths. This approach is particularly suited when the signals propagate along transmission lines with controlled geometry (e.g., parallel lands on PCBs or MCMs), but can also be applied to packages, vias, and in general to interconnection structures with complex geometry by applying suitable linear macromodeling algorithms based on some model order reduction technique. This is a very active research area, as demonstrated by the large number of recent papers on the subject (see, e.g., [1, 2, 5] and references therein). We remark that this modeling strategy is best suited for pure SI analysis since only the port behavior of the interconnection structure at few selected locations is modeled. Obviously, if the macromodel is properly derived, this port behavior includes all relevant effects including radiation losses. Consequently, this strategy can be used, e.g., for a precise characterization of some interconnection part of a system during the design stage of the active drivers and receivers, which requires a detailed knowledge of what they "see" at their terminals. However, if the near or far fields are desired for an EMC characterization of the entire structure, the port voltages and currents obtained with a circuit simulation are not sufficient. A full-wave solution must then be performed, since the distribution of the currents throughout the entire interconnection structure will affect the radiated fields.

This paper concentrates on a second complementary modeling strategy, which allows both SI and EMC analysis in a single simulation step. A conventional solver based on the well-known Finite-Difference Time-Domain (FDTD) scheme [4, 9] is used to discretize the electromagnetic fields within the computational domain, and suitable models for the nonlinear/dynamic components loading the interconnects are inserted as lumped elements within the computational mesh. We remark that the procedure for inclusion of lumped elements within the FDTD mesh has been developed by several researchers during the past ten years for standard circuit elements. For a review see [9] and references therein. Since the entire simulation is run using the main FDTD solver, all field variables are available during the simulation. This allows for susceptibility analysis (if some external incident field is applied as an additional source) and radiation analysis (through standard post-processing of transient fields computed during the FDTD simulation).

Digital ports are best represented by means of detailed transistor-level models. However, the complexity of such models can be very different according to the specific technology and application under consideration. For example, on-chip drivers may be represented by few transistors, resulting in quite simple circuits. In such cases a transistor-level simulation is affordable. On the other hand, off-chip

Proceedings of the Design,Automation and Test in Europe Conference and Exhibition (DATE'03)
1530-1591/03 $17.00 © 2003 IEEE

IEEE COMPUTER SOCIETY

transceivers for generation of signals travelling over long propagation paths at MCM or PCB level may be extremely complex and may require very long simulation times. In such cases a behavioral model is highly desirable in order to speed-up system-level simulations.

We focus here on the use of behavioral models of real-world digital I/O ports based on Radial Basis Functions (RBF) expansions [6, 7, 8]. The device is modeled through a discrete-time nonlinear dynamic parametric macromodel leading to a virtually undistinguishable response under very different loading conditions with respect to the transistor-level model. The parameters are computed only once through a rigorous identification procedure and are used for all subsequent simulations.

There are several advantages beyond accuracy in this approach. The computational cost required for the transient simulation of such a macromodel can be much less than for the transistor level circuit [6]. In addition, due to the intrinsic nature of the model representation, each device is represented by its own set of parameters. This allows the macromodel implementation to be quite general, since the same computational code can be used for very different devices simply feeding it with the proper model parameters. It is also conceivable to setup libraries of components that can be arbitrarily selected and included by the user.

The RBF macromodels used in this paper are discrete-time nonlinear models, consisting of a set of difference equations relating present and past samples of port voltage and current with fixed sampling time. The latter is usually defined in the model identification stage and is one of the key parameters that characterize the device. On the other hand, transient field solvers like FDTD often require a proper time step determined by the spatial mesh size through the Courant condition. Therefore, discrete-time macromodels can in principle be included within a FDTD mesh only if the model sampling time and the transient time step are matched. We solve this problem by presenting a resampling strategy for RBF models, which is proved to preserve time stability. We will first recall the basics of RBF parametric macromodels in Section 2, and we will discuss the hybridization with FDTD in Section 3. Numerical results and validations are presented in Section 4.

2. RBF Parametric Macromodels

We review in this section the basic definition of RBF parametric macromodels. Further details can be found in [6, 7, 8] and references therein. Let us consider the voltage and current waveforms $v(t)$ and $i(t)$ of some digital I/O port under modeling. All the macromodels considered in this paper are discrete-time models, therefore we sample the time axis with given sampling time T_s. This sampling time must be carefully determined on the basis of the dynamic features of the device. We will indicate the voltage and current samples as $v^m = v(mT_s)$, $i^m = i(mT_s)$. A general form of parametric macromodel for the device can be expressed as

$$i^m = F(\mathbf{\Theta}; \mathbf{x}_i^{m-1}, v^m, \mathbf{x}_v^{m-1}; m)\,, \tag{1}$$

where $\mathbf{x}_v^{m-1}$ and $\mathbf{x}_i^{m-1}$ are regressor vectors collecting the past r voltage and current samples,

$$\begin{aligned} \mathbf{x}_v^{m-1} &= \left[v^{m-1}, v^{m-2}, \ldots, v^{m-r}\right]^T\,, \\ \mathbf{x}_i^{m-1} &= \left[i^{m-1}, i^{m-2}, \ldots, i^{m-r}\right]^T\,. \end{aligned} \tag{2}$$

These vectors act as discrete-time internal states of the model, with r indicating its dynamic order. The function F is a nonlinear mapping from $\Re^{2r+1}$ to $\Re$ defining the *model representation* and $\mathbf{\Theta}$ is the vector of model parameters. Note that F depends also on time m, since digital drivers must be modeled as time-varying components in order to capture switching behavior. Also, we remark that Eq. (1) is suitable for the description of typical digital drivers and receivers. Nonetheless, in case of particular devices for which Eq. (1) results ill-defined, alternative forms can be conceived, e.g., by exchanging the role of port voltage and current.

In this work we mainly concentrate on model representations F based on Gaussian RBF expansions. Such representations provide approximations of the mapping F through expansion into L multivariate Gaussian functions of suitable width β centered at appropriate points $\mathbf{c}$ in the regressor space of dimension $2r+1$. A general form of such expansion can be expressed by

$$G = \sum_{l=1}^{L} \theta_l\, \Psi_l(m-1)\, \exp\left\{-\frac{(v^m - c_l^0)^2}{2\beta^2}\right\}\,, \tag{3}$$

where the term $\Psi_l(m-1)$ collects all contributions due to past voltage and current samples,

$$\Psi_l(m-1) = \exp\left\{-\frac{||\mathbf{x}_i^{m-1} - \mathbf{c}_l^i||^2 + ||\mathbf{x}_v^{m-1} - \mathbf{c}_l^v||^2}{2\beta^2}\right\}\,, \tag{4}$$

and $||\cdot||$ denotes the Euclidean norm.

The general form can be further specialized to drivers and receivers. One of the main difficulties in macromodeling output ports of drivers arises from the time-varying nature of the devices due to switching. Our proposed strategy amounts to using two separate Gaussian RBF submodels accounting for both static and dynamic effects of the port behavior at a fixed logic state, henceforth labeled i_u^m for HIGH and i_d^m for LOW state. These two submodels are time-invariant. A piecewise linear combination through time-varying weight functions $w_{u,d}^m$ provides a model for

IEEE COMPUTER SOCIETY

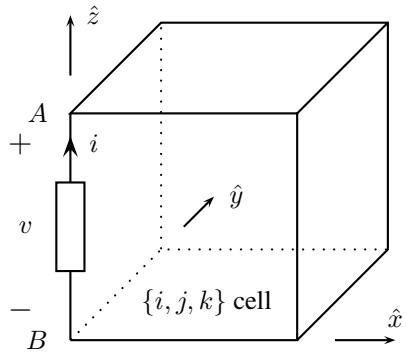

Figure 1. Collocation of the lumped element in the FDTD mesh.

the evolution of the port logic state, acting as a switch between submodels $i^m_{u,d}$, *i.e.*,

$$i^m = w^m_u i^m_u + w^m_d i^m_d \,. \tag{5}$$

Macromodeling of receivers input ports follows a similar approach. However, receivers are not time-varying components, therefore simpler models can be devised. The proposed structure for a receiver model is

$$i^m = i^m_{\rm lin} + i^m_{{\rm nl},u} + i^m_{{\rm nl},d} \tag{6}$$

where $i^m_{\rm lin}$ is a linear parametric submodel accounting for the mainly linear behavior of the port for voltage values within the range of the power supply voltage, while $i^m_{{\rm nl},u}$ and $i^m_{{\rm nl},d}$ are Gaussian RBF submodels taking into account both the nonlinear static and dynamic effects of the up and the down protection circuits, respectively.

3. Hybridization of FDTD and RBF macromodeling techniques

We consider a locally uniform medium in the vicinity of a $\hat{z}$-directed lumped element, with permettivity ε, permeability μ, and conductivity σ. The entire computational domain is discretized with a FDTD mesh size Δx, Δy, Δz along the three Cartesian coordinates (see Fig. 1). The resulting time step from Courant condition will be denoted as Δt. Note that the FDTD time step is generally unrelated to the characteristic sampling time T_s of the RBF device model to be inserted in the FDTD mesh. Therefore, we will denote the FDTD time iteration with a different index n. The current and voltage of the lumped element may be defined, respectively, as

$$i = \Delta x \Delta y \, \mathbf{J} \cdot \hat{z} \,, \qquad v = \int_{\Delta z} \mathbf{E} \cdot \hat{z} \, dz \,, \tag{7}$$

where $\mathbf{E}$ and $\mathbf{J}$ are the total electric field and the current density at the considered mesh location, indexed by $\{i,j,k\}$. The expression of the discretized Maxwell-Ampere curl equation modified to account for the lumped element with split incident and scattered fields (subscripts $\{i,s\}$, respectively) reads [4, 9]

$$\alpha_0 v^{n+1} - \alpha_1 v^n + \alpha_2 \left[\hat{z} \cdot \nabla \times \mathbf{H}_s\right]^{n+1/2}_{ijk} + \alpha_2 \varepsilon_0 \left.\frac{\partial E_{i,z}}{\partial t}\right|^{n+1/2}_{ijk} - \alpha_3 \left(i^{n+1} + i^n\right) = 0 \,, \tag{8}$$

where

$$\alpha_0 = 1 + \frac{\sigma \Delta t}{2\varepsilon} \,, \tag{9}$$

$$\alpha_1 = 1 - \frac{\sigma \Delta t}{2\varepsilon} \,, \tag{10}$$

$$\alpha_2 = \frac{\Delta z \Delta t}{\varepsilon} \,, \tag{11}$$

$$\alpha_3 = \frac{\Delta z \Delta t}{2\varepsilon \Delta x \Delta y} \,. \tag{12}$$

Equation (8) must be coupled with the $i - v$ port characteristic of the lumped element, which is expressed by Eq. (1). However, care must be taken in case the time step T_s characteristic of the RBF model is different from the time step Δt induced by the FDTD mesh size. Actually, the latter is much smaller than T_s for typical structures found in the applications. This problem may be solved by a resampling procedure of the RBF model. First, the discrete-time RBF model is converted into a continuous-time model using a forward finite-difference approximation. Then, the continuous-time model is resampled with the FDTD time step Δt, using the same forward finite-difference approximation. A straightforward derivation leads to the general expression

$$\begin{aligned} \mathbf{x}^{n+1}_i &= \mathbf{Q}\,\mathbf{x}^n_i + \tau\,\mathbf{e}_r\,F(\boldsymbol{\Theta}; \mathbf{x}^n_i, v^n, \mathbf{x}^n_v; n) \,, \\ \mathbf{x}^{n+1}_v &= \mathbf{Q}\,\mathbf{x}^n_v + \tau\,\mathbf{e}_r\,v^n \,, \\ i^n &= F(\boldsymbol{\Theta}; \mathbf{x}^n_i, v^n, \mathbf{x}^n_v; n) \,, \end{aligned} \tag{13}$$

where the time step of the RBF model is now Δt. Matrix $\mathbf{Q}$ is banded with non vanishing elements $q_{ii} = 1 - \tau$ and $q_{i,i-1} = \tau$, with $\tau = \Delta t / T_s$, and $\mathbf{e}_r = (1, 0, \ldots, 0)^T$. This system can be solved at each time step through the Newton-Raphson algorithm.

This modeling strategy has two remarkable features. First, the time-domain conversion preserves time stability. A complete proof is detailed in Section 3.1. Second, the RBF model representation F is generally quite smooth and well-behaved, while the inverse of the Jacobian matrix of system (8)-(13) can be computed analytically. As a consequence, the Newton-Raphson iterations required for convergence at each time iterations are very few. We remark

IEEE COMPUTER SOCIETY

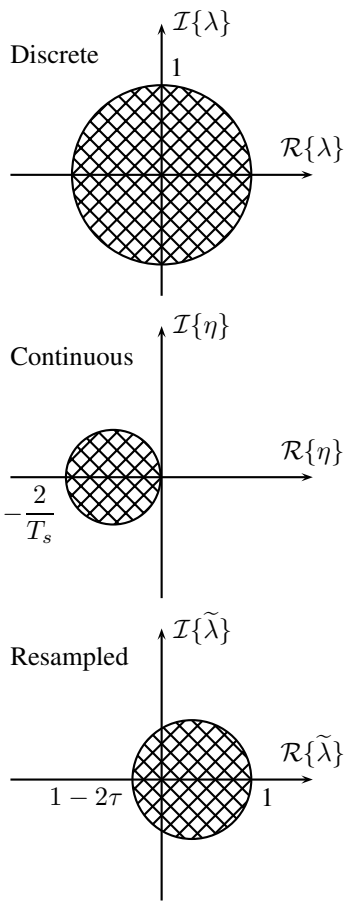

Figure 2. Stability of the time conversion applied to the linear test problem. The three panels show the eigenvalues of the discrete, continuous, and resampled test problem.

that this smoothness is controlled by choosing an appropriate sampling time T_s for the RBF model during the identification stage. Therefore, the nonlinearity is weak by construction for the entire class of devices herewith considered. Note that this is true also for state-of-the-art fast digital drivers and receivers for very high speed applications. Illustrative numerical examples are provided in next section.

3.1. Resampling and stability

This section investigates the time stability of the resampled macromodels above described. We show in the following that the time conversion steps leading to the resampled model preserve stability. Therefore, if the original macromodel is stable, also the resampled one will be stable.

Stability of resampling is best illustrated by the behavior of a standard test problem, namely

$$\widehat{\zeta}^{m+1} = \lambda\,\widehat{\zeta}^{m}, \qquad |\lambda| < 1\,. \tag{14}$$

The results presented in [3] show that the above test problem is appropriate since all the eigenvalues associated to the original RBF model before resampling have magnitude less than one, i.e., the criterion on λ is unconditionally satisfied. If we now apply the proposed discrete-to-continuous time conversion procedure we get

$$\frac{\mathrm{d}}{\mathrm{d}t}\zeta(t) = \eta\,\zeta(t)\,, \qquad \eta = \frac{\lambda - 1}{T_s}\,, \tag{15}$$

where a first-order forward approximation of the time derivative has been used. The relationship between discrete and continuous state variables is $\zeta(mT_s) \simeq \widehat{\zeta}^{m}$ with first-order accuracy. Due to the stability constraint on the original system (14) we conclude that the eigenvalue η of the continuous system has negative real part, allowing us to prove stability. Applying now the continuous-to-discrete time approximation with sampling time Δt, and using again a first-order forward difference approximation, we get the resampled system

$$\widetilde{\zeta}^{n+1} = \widetilde{\lambda}\,\widetilde{\zeta}^{n}\,, \qquad \widetilde{\lambda} = 1 + \tau(\lambda - 1)\,. \tag{16}$$

Figure 2 depicts the region of the complex plane with possible values of $\widetilde{\lambda}$, i.e., a circle centered at $(1-\tau)$ with radius τ. Stability is guaranteed when $|\widetilde{\lambda}| < 1$, i.e., when the resampling factor satisfies

$$\tau \leq 1\,. \tag{17}$$

This is quite natural since the overall resampling process can be interpreted as the application of a linear interpolation scheme. If the resampling factor becomes larger than one this scheme becomes an extrapolation, which is always to be avoided. Also, due to the usual size of the interconnect structures where the devices under investigation can be found, the required cell size for FDTD must be very small in order to describe the geometry with sufficient accuracy. Therefore, the resulting time step Δt is generally much smaller than the time scale of typical driver/receiver responses. We conclude that the requirement of Eq. (17) is not restrictive in any case of practical interest.

4. Numerical Results

The first example is intended to validate the mixed RBF-FDTD modeling procedure. The structure that we chose for validation is a simple transmission line depicted in Fig. 3. The computational domain is $180 \times 24 \times 23$ cells, with mesh size $\Delta x = \Delta y = \Delta z = 0.723$ mm, and is terminated

IEEE COMPUTER SOCIETY

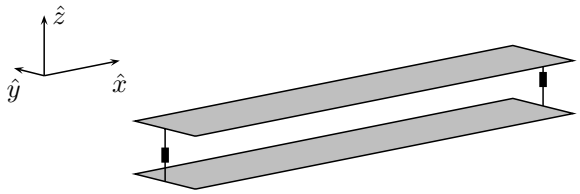

Figure 3. Transmission line structure used for validation.

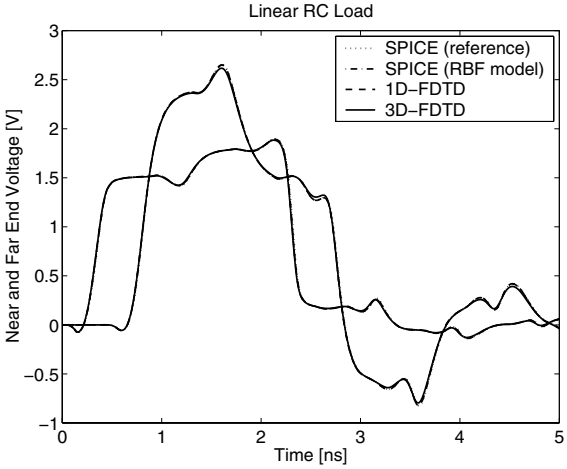

Figure 4. Termination voltages for the transmission line structure with switching driver at near end and with a RC load at the far end.

by absorbing boundary conditions. The strips are implemented as zero-thickness conductors and are 4 cells wide and 160 cells long. The separation between the two strips is 3 cells. The effective characteristic impedance of the resulting transmission line is $Z_c \sim 131\,\Omega$, while the line delay is $T_D \sim 0.4$ ns. The line is excited at the near end by the lumped RBF macromodel of a commercial device, namely a high-speed CMOS driver (power supply: $V_{ss} = 0\,\mathrm{V}$, $V_{dd} = 1.8\,\mathrm{V}$) used in IBM mainframe products. The driver forces a bit pattern `'010'` at its output port, with a bit time of 2 ns. The far end termination is varied in order to illustrate load insensitivity of the proposed modeling strategy. In particular, we consider both a linear capacitive load (shunt connection of a 1 pF capacitor and a 500 Ω resistor) and a RBF macromodel of a receiver (same technology as the driver). The simulation results are depicted in Figures 4 and 5. All the different curves are very consistent, although they have been computed using very different simulation engines. Namely: (*i*) SPICE with ideal TL and transistor-level models of the devices; (*ii*) SPICE with ideal TL and RBF models of the devices; (*iii*) 1D-FDTD for the TL and

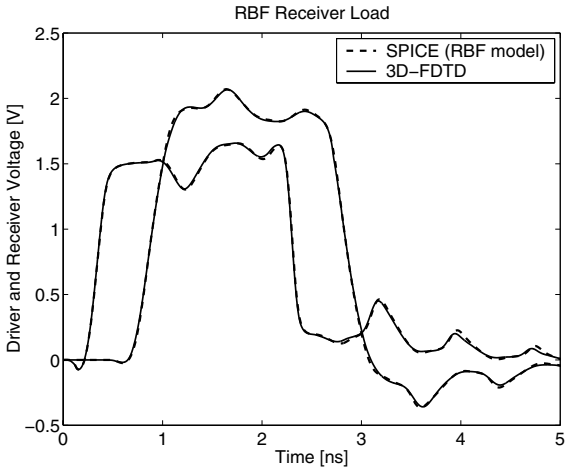

Figure 5. Termination voltages for the transmission line structure with switching driver at near end and with a RBF receiver load at the far end.

RBF models of the devices; (*iv*) 3D-FDTD for the TL and RBF models of the devices. Only the 3D-FDTD result has a marginal deviation from the other curves due to numerical dispersion. We remark that the number of Newton-Raphson iterations required to solve the RBF model equations never exceeded a maximum number of three, whereas the accuracy threshold was set to the very stringent value of 10^{-9}.

We turn now to a more realistic application. The 5 cm $\times$ 5 cm PCB structure depicted in Fig. 6 is considered. This configuration is similar to the one analyzed in [2]. Three 400 μm-wide coupled strips run parallel to each other on the top (along x coordinate, length 4 cm) and bottom (along y coordinate, length 4 cm) of the PCB signal layer. Three vias connect the orthogonal sections of the strips. Top and bottom glue layers cover the signal layer, and the entire PCB is metallized on both sides. The relative permettivity for all layers is $\varepsilon_r = 4.3$, with a single layer height of 400 μm. The innermost strip is driven by the RBF macromodel of the driver on one end and is terminated on the other end by the RBF macromodel of the receiver. All the other terminations consist of 50 Ω resistors. The driver forces a `'010'` bit sequence at its output port. In addition, an external wave Gaussian pulse impinges on the structure from a direction $\{\theta = 90^o, \varphi = 180^o\}$ with θ-polarized electric field in standard spherical coordinates. The amplitude of the pulse is 2kV/m, with a bandwidth of 9.2 GHz. Fig. 6 shows the termination voltages for the driven line with and without incident field. This example illustrates that the proposed modeling strategy can be effectively employed for the complex task of predicting incident-field coupling effects on interconnected networks

IEEE COMPUTER SOCIETY

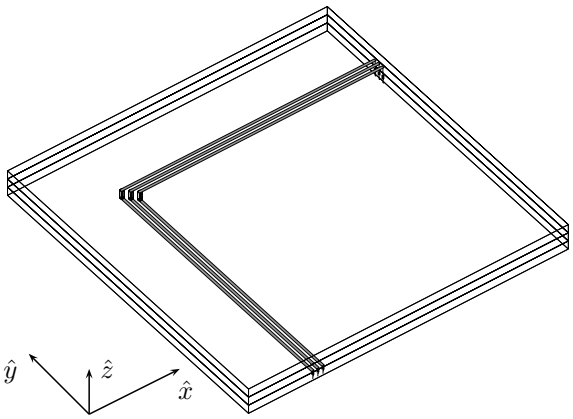

Figure 6. PCB structure for illustration of incident field coupling.

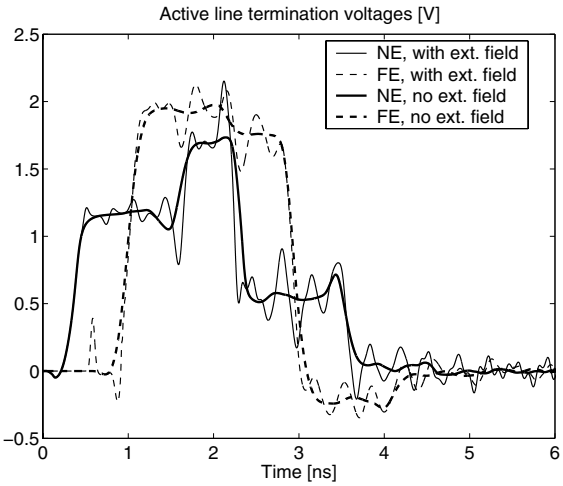

Figure 7. Termination voltages with and without incident field contribution (NE, near end; FE, far end).

loaded by real-world components.

5. Conclusions

We have presented an effective strategy for the full-wave modeling of interconnected structures loaded by real-world components like digital drivers and receivers. The complex nonlinear and dynamic behavior of such devices is modeled using approximate behavioral models based on Radial Basis Functions (RBF) expansions. These are discrete-time parametric models, capable of reproducing with very high accuracy the port behavior of the devices. A discrete-time resampling strategy has been presented in order to allow the direct insertion of a RBF behavioral model within the computational mesh of a standard field solver based on finite differences. The presented numerical results confirm the high degree of accuracy of the method.

References

[1] A. Dounavis, E. Gad, R. Achar, M. Nakhla, "Passive model reduction of multiport distributed interconnects", *IEEE Trans. Microwave Theory and Tech.*, **48**, 2000, 2325–34.

[2] I. Erdin, M. Nakhla, R. Achar, "Circuit Analysis of Electromagnetic Radiation and Field Coupling Effects for Networks with Embedded Full-Wave Modules", *IEEE Trans. Electromaget. Compat.*, **42**, 2000, 449–460.

[3] S. Grivet-Talocia, I. Stievano, F. Canavero, "Hybridization of FDTD and Device Behavioral-Modeling Techniques", *IEEE Trans. EMC*, Feb. 2003, in press.

[4] K. S. Kunz, R. J. Luebbers, "The Finite-Difference Time-Domain Method for Electromagnetics", Boca Raton, FL: CRC Press, 1994.

[5] A. Odabasioglu, M. Celik, L. T. Pileggi, "PRIMA: passive reduced-order interconnect macromodeling algorithm," *IEEE Trans. Computer-Aided Design of Int. Circ. and Sys.*, **17**, 1998, 645–654.

[6] I. S. Stievano, F. G. Canavero, I. A. Maio, "Parametric Macromodels of Digital I/O Ports," *IEEE Trans. Advanced Packaging*, Vol. 25, N. 2, May 2002, pp. 255–264.

[7] I. S. Stievano, Z. Chen, D. Becker, F. G. Canavero, G. Katopis, I. A. Maio, "Macromodeling of Digital I/O Ports for System EMC Assessment", Proc. of *Design, Automation and Test in Europe Conference, DATE,* Paris, F, Mar. 4–8, 2002.

[8] I. S. Stievano, I. A. Maio, "Behavioral models of digital IC ports from measured transient waveforms," Proc. of 9^{th} *IEEE Topical Meeting on Electrical Performance of Electronic Packaging, EPEP,* Scottsdale, AZ, pp. 211–214, Oct. 23–25, 2000.

[9] A. Taflove (ed.), *Advances in Computational Electrodynamics: The Finite-Difference Time-Domain Method*, Norwood, MA: Artech House, 1998.

IEEE COMPUTER SOCIETY